

Fibronectin in cell adhesion and migration via N-glycosylation

SUPPLEMENTARY MATERIALS

Supplementary Table 1: The comparison of the amino acid sequences between homo and porcine fibronectin. .

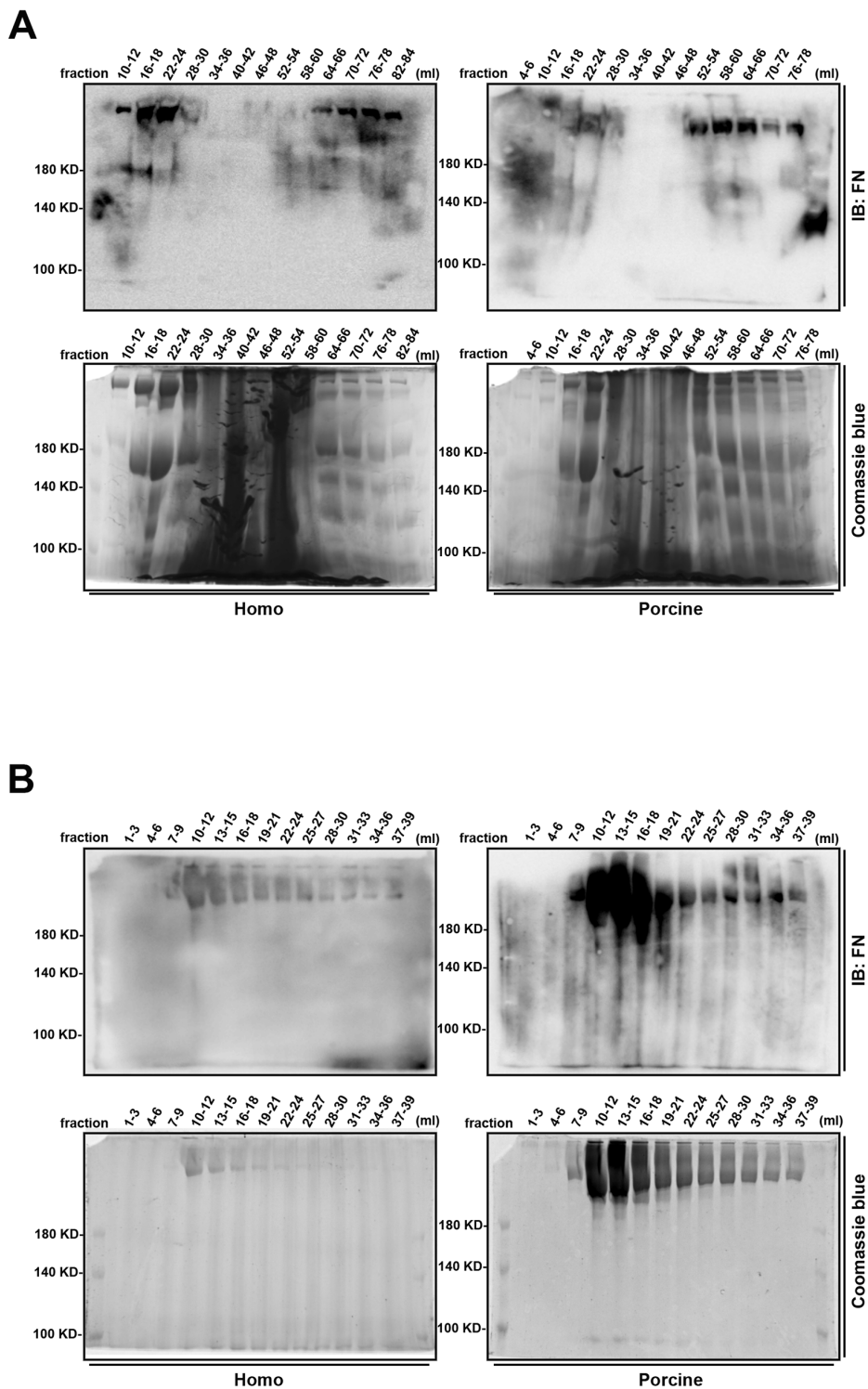
See Supplementary File 1

Supplemental Table 2: The list of identified glycopeptides from homo plasma fibronectin.

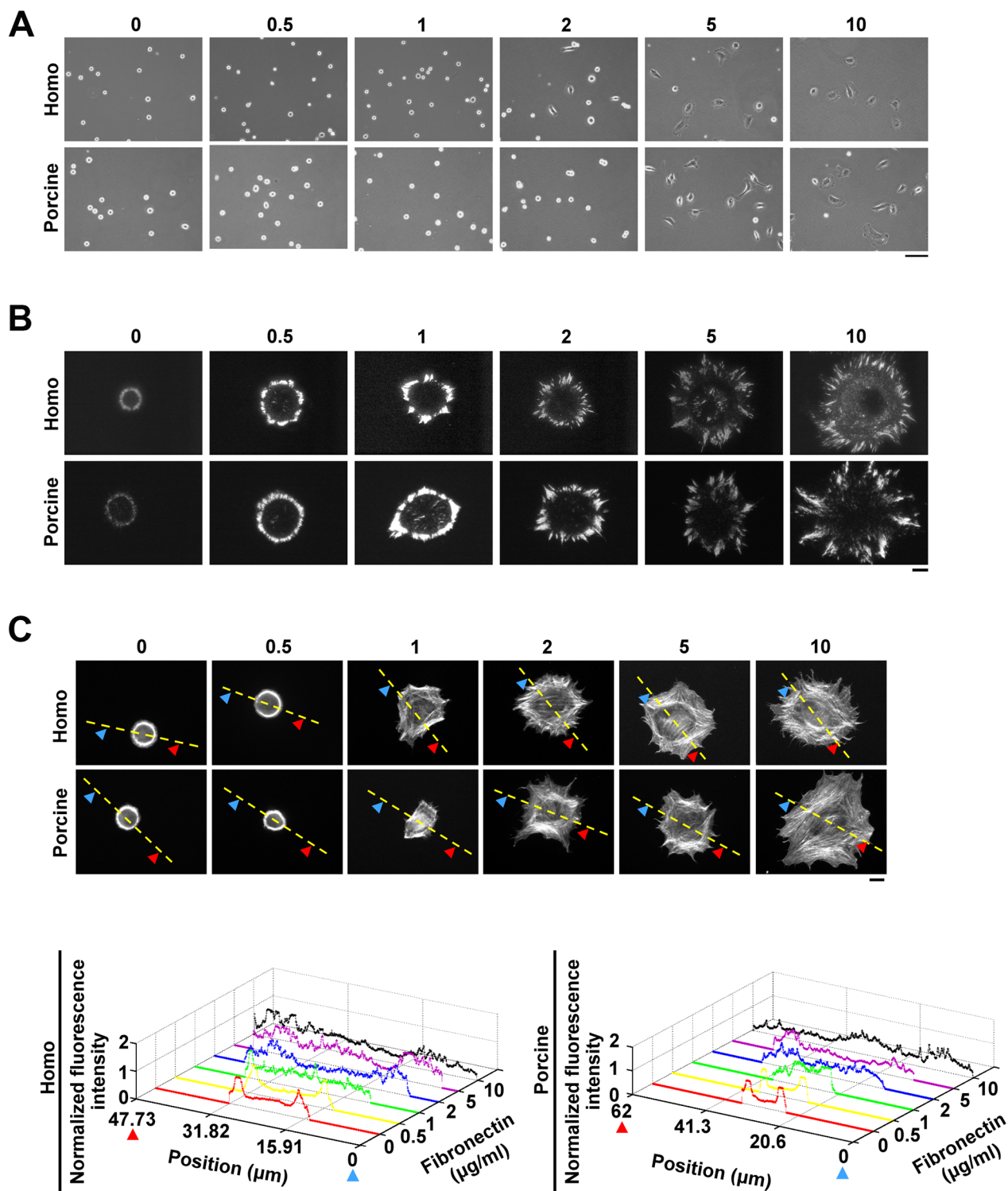
See Supplementary File 2

Supplemental Table 3: The list of identified glycopeptides from porcine plasma fibronectin.

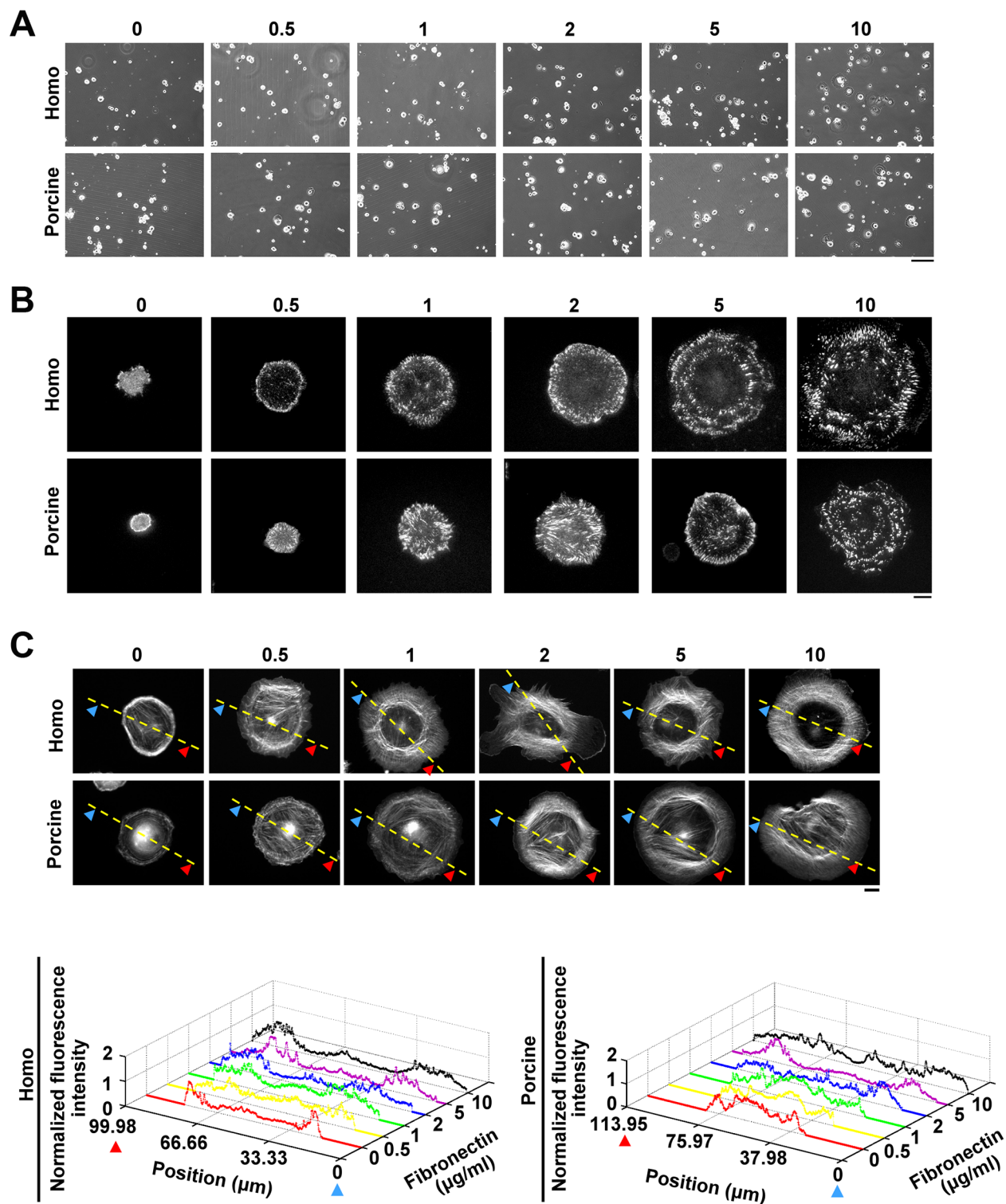
See Supplementary File 3



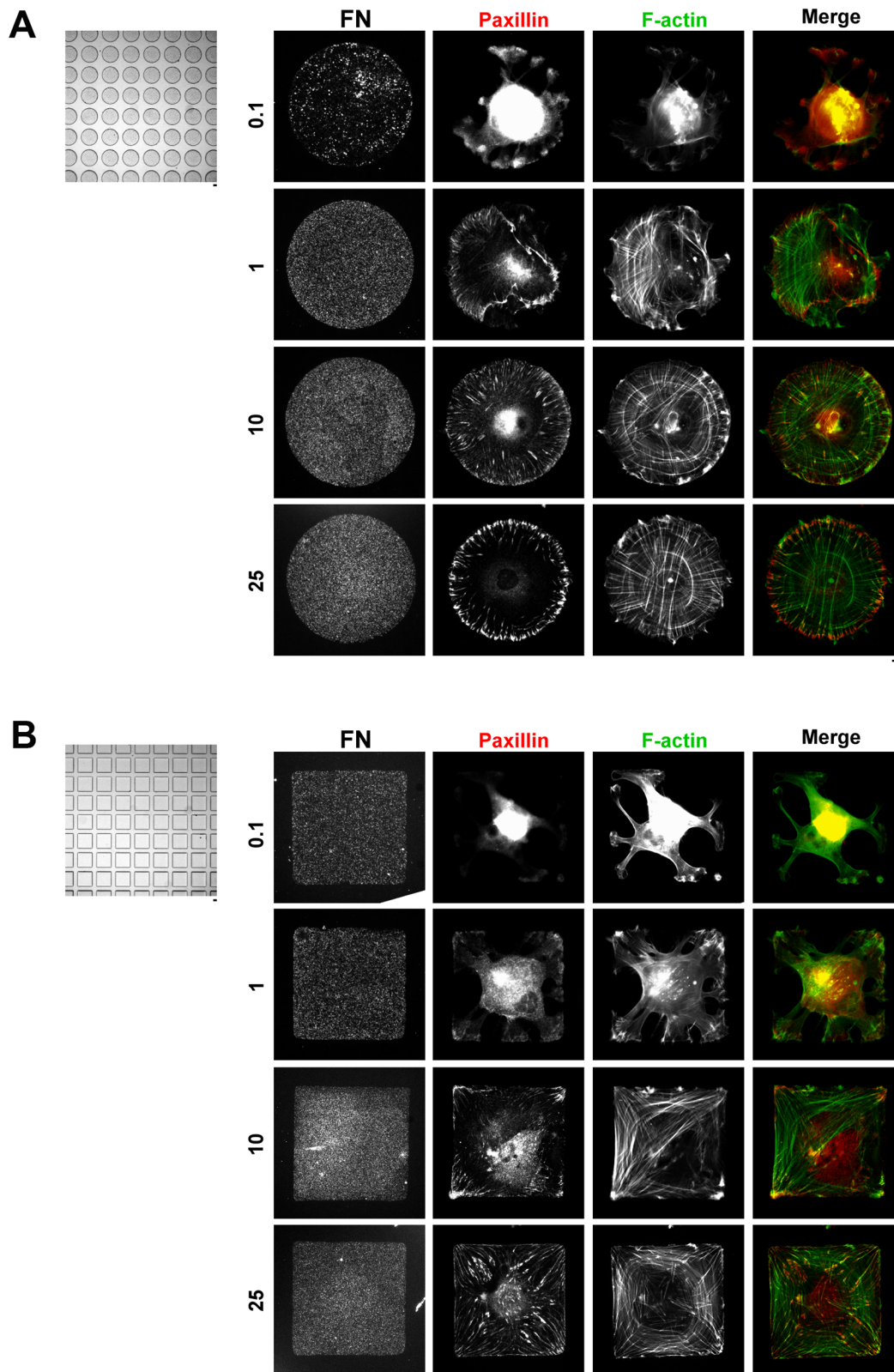
Supplementary Figure 1: Sequential separation of the two fibronectins from homo and porcine plasma. (A) The fractions of the flow-through materials that had passed through the Sepharose CL-4B column were analyzed by Western blotting using antibodies against fibronectin (FN) and by Coomassie blue staining. (B) The fractions of the eluted materials that obtained from the gelatin-Sepharose Fast Flow 4B column using 1M Arginine were analyzed by Western blotting using antibodies against fibronectin (FN) and by Coomassie blue staining.



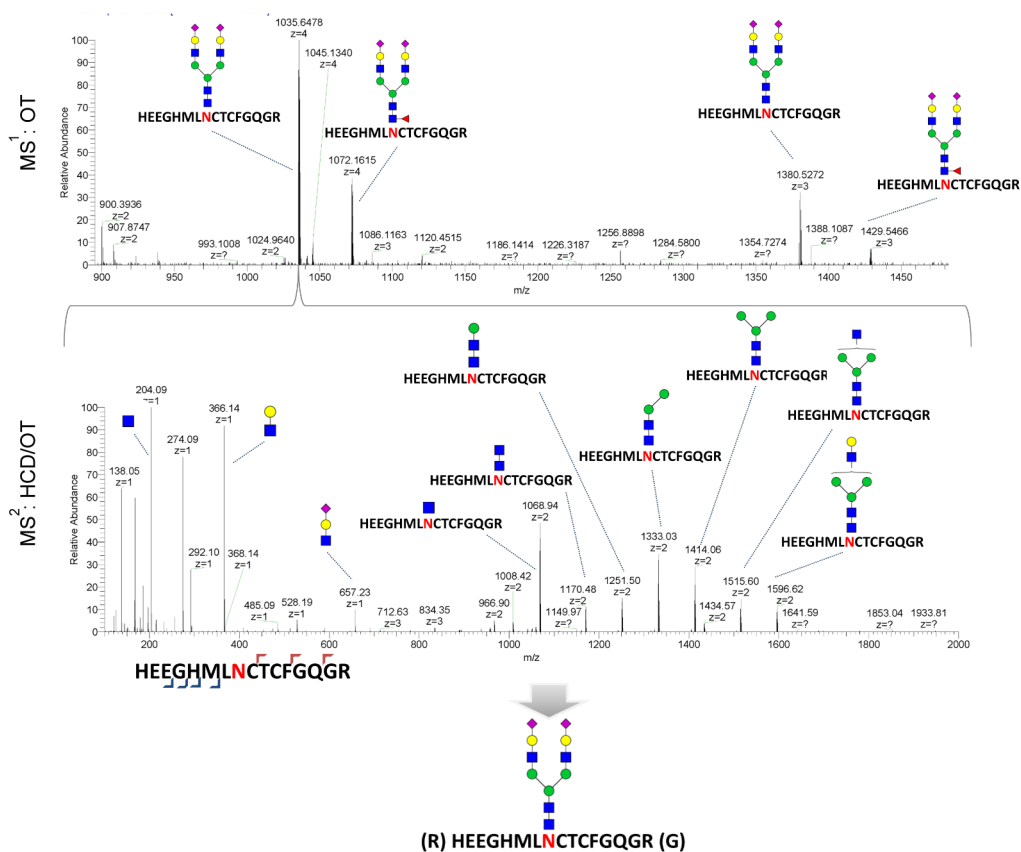
Supplementary Figure 2: Cell adhesion in response to homo and porcine plasma fibronectin using HeLa cells. (A) HeLa cells 30 min after plating on coverslips coated with the indicated fibronectin concentration ($\mu\text{g/ml}$). Bar, 100 μm . (B) TIRFM images of the HeLa cells 1.5 h after plating on coverslips coated with the indicated fibronectin concentration immunostained with paxillin. Bar, 10 μm . (C) Confocal images of HeLa cells 1.5 h after plating on coverslips coated with the indicated fibronectin concentration ($\mu\text{g/ml}$). Bar, 10 μm . (Bottom) Relative fluorescence intensity taken along the line highlighted in the confocal image with the edge marked with arrows and distance.



Supplementary Figure 3: Cell adhesion in response to homo and porcine plasma fibronectin using HFF1 cells. (A) HFF1 cells 30 min after plating on coverslips coated with the indicated fibronectin concentration ($\mu\text{g/ml}$). Bar, 100 μm . (B) TIRFM images of HFF1 cells 1.5 h after plating on coverslips coated with the indicated fibronectin concentration immunostained with paxillin. Bar, 20 μm . (C) Confocal images of HFF1 cells 1.5 h after plating on coverslips coated with the indicated fibronectin concentration ($\mu\text{g/ml}$). Bar, 10 μm . (Bottom) Relative fluorescence intensity taken along the line highlighted in the confocal image with the edge marked with arrows and distance.



Supplementary Figure 4: Cell adhesion in response to homo and porcine plasma fibronectin using various different pattern shapes. (A) Confocal images of mesenchymal stem cells that were spreading on the circular micropattern (10,000 μm^2) coated with the indicated fibronectin concentration ($\mu\text{g}/\text{ml}$), and stained with paxillin (red) and F-actin (green). Bar, 10 μm . (B) Confocal images of the mesenchymal stem cells that had spread on the square micropattern (10,000 μm^2) coated with the indicated fibronectin concentration ($\mu\text{g}/\text{ml}$), and stained with paxillin (red) and F-actin (green). Bar, 10 μm .



Supplementary Figure 5: LC-MS/MS-based glycopeptide sequencing and identification. (Top) A combined MS profile from scans acquired across the elution time span shows two different glycoforms, with their m/z values and charge states in the spectrum magnified for the mass range m/z 900-1500. (Bottom) A glycopeptide HCD-MS² spectrum for one identified glycoform is shown as an example. The Y1 ion at m/z 1068.94/2⁺ for the peptide core contains the implicated N-glycosylation site N542, with glycan combination.